

# Influence of Inelastic Collisions with Hydrogen Atoms on Non-LTE Oxygen Abundance Determination in the Sun and late-type stars

T. M. Sitnova <sup>\*1,2</sup> L. I. Mashonkina<sup>1</sup>

<sup>1</sup> *Institute of Astronomy, Russian Academy of Sciences, Moscow, Russia*

<sup>2</sup> *Herzen State Pedagogical University, St. Petersburg, Russia*

## Abstract

We present the non-local thermodynamic equilibrium (non-LTE) calculations for O I with the updated model atom that includes quantum-mechanical rate coefficients for O I + H I inelastic collisions from the recent study of Barklem (2018). The non-LTE abundances from the O I lines were determined for the Sun and 46 FG stars in a wide metallicity range,  $-2.6 < [\text{Fe}/\text{H}] < 0.2$ . An application of accurate atomic data leads to larger departures from LTE and lower oxygen abundances compared to that for the Drawin's theoretical approximation. For the infrared O I 7771-5 Å triplet lines, the change in the non-LTE abundance is  $-0.11$  dex for the solar atmospheric parameters and decreases in absolute value towards lower metallicity. We revised the  $[\text{O}/\text{Fe}]$ - $[\text{Fe}/\text{H}]$  trend derived in our earlier study. The change in  $[\text{O}/\text{Fe}]$  is small in the  $[\text{Fe}/\text{H}]$  range from  $-1.5$  to  $0.2$ . For stars with  $[\text{Fe}/\text{H}] < -1$ , the  $[\text{O}/\text{Fe}]$  ratio has increased such that  $[\text{O}/\text{Fe}] = 0.60$  at  $[\text{Fe}/\text{H}] = -0.8$  and increases up to  $[\text{O}/\text{Fe}] = 0.75$  at  $[\text{Fe}/\text{H}] = -2.6$ .

## 1 Introduction

The oxygen abundance in the atmospheres of the Sun and stars is an important quantity for testing the Galactic chemical evolution scenarios and the theory of stellar structure and evolution.

The infrared (IR) O I 7771-5 Å triplet lines are the only set of atomic lines observed in spectra of metal-poor stars. Previously, many authors have shown that the IR O I lines are formed under conditions far from local thermodynamic equilibrium (LTE). The oxygen NLTE abundance was first determined by Kodaira and Tanaka (1972) and Johnson (1974) for stars and by Shchukina (1987) for the Sun. Subsequently, more comprehensive oxygen model atoms were constructed by Kiselman (1991), Carlsson and Judge (1993), Takeda (1992), Paunzen et

---

\*sitnova@inasan.ru

al. (1999), Reetz (1999), Mishenina et al. (2000), and Przybilla et al. (2000). Non-LTE leads to a strengthening of O I IR lines and, consequently, to a decrease in the abundance derived from these lines.

Having considered atomic and molecular lines in the solar spectrum, Asplund et al. (2004) achieved agreement between the abundances from different lines using a three-dimensional (3D) model atmosphere based on hydrodynamic calculations and the non-LTE corrections calculated with a classical 1D model atmosphere. In Asplund et al. (2004), the mean abundance from atomic and molecular lines is  $\log \varepsilon = 8.66 \pm 0.05^1$ ; further, Asplund et al. (2009) obtained  $\log \varepsilon = 8.69$  by the same method. This value turned out to be lower than  $\log \varepsilon = 8.93 \pm 0.04$  obtained previously by Anders and Grevesse (1989) from OH molecular lines using the semi-empirical HM74 model atmosphere (Holweger and Mueller 1974). It is worth noted that the models of solar internal structure constructed with the chemical composition from Anders and Grevesse (1989) described well the sound speed and density profiles inferred from helioseismological observations. A revision of the oxygen abundance by 0.27 dex led to a discrepancy between the theory and observations up to  $15\sigma$  (Bahcall and Serenelli 2005). This problem still remains unsolved.

In our previous paper (Sitnova et al. 2013), based on the model atom from Przybilla et al. (2000) improved by including rate coefficients for electron-impact excitation of O I from Barklem (2007), we derived the mean oxygen abundance  $\log \varepsilon = 8.74 \pm 0.05$  from the O I 6300, 6158, 7771-5, and 8446 Å lines in the solar spectrum using a classical plane-parallel solar model atmosphere and  $\log \varepsilon_{+3D} = 8.78 \pm 0.03$  by applying the 3D corrections from the Caffau et al. (2008).

There is a huge number of studies where the [O/Fe] ratio was determined for samples of stars; here, we mention some of them. It is well known from observations that stars with  $[\text{Fe}/\text{H}]^2 < 0$  show positive [O/Fe] ratio, which increases with decreasing metallicity approximately down to  $[\text{Fe}/\text{H}] \simeq -1$  and then remains almost constant at  $[\text{Fe}/\text{H}] < -1$ . The [O/Fe] ratio as a function of [Fe/H] is well-understood qualitatively and quantitatively, and, in general, the Galactic chemical evolution models describe the observational data for [O/Fe]. Almost the same [O/Fe] ratio for stars with  $[\text{Fe}/\text{H}] < -1$  stems from the fact that, at the epoch of their formation, the interstellar gas was enriched with metals by massive stars exploded as type II supernovae (SNe II) or hypernovae. By the formation epoch of stars with  $[\text{Fe}/\text{H}] \simeq -1$ , type Ia supernovae began to contribute to the enrichment of the medium with heavy elements, where the iron production efficiency is higher than that in the explosions of massive stars, which led to a decrease in [O/Fe]. At present, attempts are being made to establish subtle features in the behavior of [O/Fe], for example, to understand what the actual spread in [O/Fe] is for stars with a similar metallicity, from which the conclusion about the mixing of matter in the Galaxy can be drawn. Such an attempt was made by Bertran de Lis et al. (2016), who determined the oxygen abundance from IR OH lines in red giants with metallicity  $-0.65 < [\text{Fe}/\text{H}] < 0.25$ . Ramírez et al. (2013) determined the oxygen abundance by taking into account the departures from LTE from the O I 7771–5 Å lines for a sample of several hundred FGK dwarfs with  $-1.2 < [\text{Fe}/\text{H}] < 0.4$ . Bensby et al. (2014) performed a detailed analysis of 13 elements from

---

<sup>1</sup>Here,  $\log \varepsilon = \log(N_{\text{elem}}/N_{\text{H}}) + 12$ .

<sup>2</sup>We use the standard notation for the elemental abundance ratios  $[\text{X}/\text{H}] = \log(N_{\text{X}}/N_{\text{H}})_{\text{star}} - \log(N_{\text{X}}/N_{\text{H}})_{\text{Sun}}$

oxygen to barium in several hundred nearby dwarf stars with  $-2.6 < [\text{Fe}/\text{H}] < 0.4$ . The oxygen abundance was inferred from the O I 7771–5 Å lines in non-LTE. In these papers, particular attention is given to the chemical peculiarities of stars in various Galactic subsystems (the thin and thick disks, the halo, the Hercules and Arcturus streams). Amarsi et al. (2015) collected data from the literature on oxygen abundance determinations over 2000–2015 for dwarf stars with  $-3.3 < [\text{Fe}/\text{H}] < 0.5$ , redetermined their atmospheric parameters using the temperatures from the IR flux method, and corrected the derived abundance by applying the corrections for the hydrodynamic and non-LTE effects. As a result, the authors found a linear increase in  $[\text{O}/\text{Fe}]$  from  $-0.3$  to  $0.6$  as  $[\text{Fe}/\text{H}]$  decreased from  $0.5$  to  $-0.7$  and then a constant  $[\text{O}/\text{Fe}]$  down to  $[\text{Fe}/\text{H}] \simeq -2.5$ ; with a possible increase in  $[\text{O}/\text{Fe}]$  to  $0.8$  at lower metallicity. The question of whether there is an increase in  $[\text{O}/\text{Fe}]$  at  $[\text{Fe}/\text{H}] < -1$  is not completely clear. There are different opinions on that score in the literature. For example, from analysis of OH lines, Israelian et al. (1998) found a linear increase in  $[\text{O}/\text{Fe}]$  from  $0.6$  to  $1$  for  $[\text{Fe}/\text{H}]$  from  $-1.5$  to  $-3$ . Fulbright and Johnson (2003) also found an increase in  $[\text{O}/\text{Fe}]$  from  $0.6$  to  $0.8$  as  $[\text{Fe}/\text{H}]$  decreased from  $-1$  to  $-2.5$  using the forbidden 6300 Å line and the IR 7771-5 Å triplet lines. However, the results of Tomkin et al. (1992), Gratton et al. (2000), Nissen et al. (2002), Cayrel et al. (2004), Fabbian et al. (2009), Sitnova (2016), and Zhao et al. (2016), which are also based on an analysis of atomic O I lines, suggest a constant  $[\text{O}/\text{Fe}]$  ratio at  $[\text{Fe}/\text{H}] < -1$ .

For the Sun and cool stars, the non-LTE abundance derived from the atomic lines can be inaccurate due to the uncertainty in the statistical equilibrium calculations related to the lack of knowledge of the excitation and ionization efficiencies in inelastic collisions with neutral hydrogen. Quantum-mechanical calculations of collisions with hydrogen atoms are available for a number of atoms: for Li I (Belyaev and Barklem 2003), Na I (Belyaev et al. 1999, 2010; Barklem et al. 2010), Mg I (Barklem et al. 2012), Al I (Belyaev 2013), Si I (Belyaev et al. 2014), K I (Belyaev and Yakovleva 2017), and Ca I (Belyaev et al. 2016; Barklem 2016; Mitrushchenkov et al. 2017). For those atoms, where accurate calculations or laboratory measurements are missing, the rates of inelastic collisions with H I are calculated from the formula derived by Steenbock and Holweger (1984) using the formalism of Drawin (1968, 1969). The authors themselves estimate the accuracy of the formula to be one order of magnitude. A scaling factor ( $S_{\text{H}}$ ) that can be found empirically by reconciling the abundances from lines with strong and weak departures from LTE is usually introduced in this formula. For oxygen, Allende Prieto et al. (2004) and Pereira et al. (2009) obtained  $S_{\text{H}} = 1$  by investigating the changes of the center-to-limb variation of O I line profiles in solar intensity spectrum; Takeda (1995) obtained the same result from O I lines in the solar spectrum in fluxes. For the Sun and cool stars, agreement between the abundances determined from different O I lines can be achieved by choosing the scaling factor. Caffau et al. (2008) performed non-LTE calculations for O I with  $S_{\text{H}} = 0, 1/3$ , and  $1$ . The higher the efficiency of collisions with hydrogen atoms leads to the smaller departures from LTE and the higher abundance. For example, for the IR O I 7771 Å line the abundance derived with  $S_{\text{H}} = 1$  is higher than that with  $S_{\text{H}} = 0$  by  $0.12$  dex. It is important to note that Belyaev and Yakovleva (2017) proposed a simplified but physically realistic method of estimating the rates of inelastic collisions with hydrogen atoms that is recommended to be applied instead of Drawin’s approximation for those elements where accurate data are not available so far.

This study was motivated by the appearance of quantum-mechanical rate coefficients for O I + H I inelastic collisions performed by Barklem (2018). In this paper, we check how the use of data from Barklem (2018) affects the oxygen abundance determination for the Sun and a sample of FG stars with metallicity  $-2.6 < [\text{Fe}/\text{H}] < 0.2$  and on the  $[\text{O}/\text{Fe}]$ – $[\text{Fe}/\text{H}]$  trend derived in our earlier study (Zhao et al. 2016). The model atom and the methods and codes used are described in Section 2. The O I lines in the Sun are analyzed in Section 3. Stellar atmospheric parameters, observations, and the derived oxygen abundance are described in Section 4. Our results are presented in the Conclusions.

## 2 Method of oxygen abundance determination

We determined the oxygen abundance from O I lines in the non-LTE case where the population of each level in a model atom is calculated by simultaneously solving the system of statistical equilibrium (SE) and radiative transfer equations. To solve this system of equations in a specified model atmosphere, we use the DETAIL code developed by Butler and Giddings (1985) based on the accelerated  $\Lambda$ -iteration method. The opacity calculation was improved, as described by Mashonkina et al. (2011). The level populations obtained in DETAIL were then used to compute the line profiles with the synthV\_NLTE code (Tsymbal 1996, updated in Ryabchikova et al. 2016). We use O. Kochukhov’s binmag<sup>3</sup> code to fit the theoretical spectrum with the observed one.

The technique of our calculations and the mechanism of departures from LTE for O I were described in Sitnova et al. (2013). We use the multilevel model atom constructed from the most up-to-date atomic data. We adopted the model atom from Przybilla et al. (2000) as a basis; it consists of 51 O I levels and the O II ground state. The level energies were taken from NIST (Kramida et al. 2015); the transition oscillator strengths and photoionization cross sections were taken from the Opacity Project (Seaton et al. 1994), which are accessible in the TOPbase<sup>4</sup> database. To calculate the rates of bound-bound transitions in collisions with electrons, we use the quantum-mechanical calculations from Barklem (2007) for 153 transitions. For the remaining transitions, where there are no accurate data, we use the formulas from van Regemorter (1962) and Wooley and Allen (1948) for optically allowed and forbidden transitions, respectively. To calculate the rates of bound-free transitions in collisions with electrons, we use the formula from Seaton (1962) with the threshold photoionization cross section from TOPbase. The resonant charge exchange ( $\text{O I} + \text{p} \leftrightarrow \text{O II} + \text{H I}$ ) was taken into account as prescribed by Arnaud and Rothenflug (1985). In this study, we take into account the excitation/deexcitation and ion-pair formation/mutual neutralization processes in collisions with hydrogen atoms according to the data from Barklem (2018). Previously, we used Drawin’s approximation (Drawin 1968, 1969; Steenbock and Holweger 1984) due to the absence of accurate data. Figure 1 shows the transition rates in inelastic collisions with hydrogen atoms and electrons under conditions typical for the solar atmosphere at the O I line formation depths. According to the data from Barklem (2018), the O I + H I excitation rates are systematically lower than those calculated

---

<sup>3</sup><http://www.astro.uu.se/~oleg/download.html>

<sup>4</sup><http://cdsweb.u-strasbg.fr/topbase/topbase.html>

from Drawin’s formula. On average, the difference between the rates is about two orders of magnitude. For transitions with energies  $\Delta E = E_u - E_l < 1.5$  eV Barklem’s rates for O I + H I collisions are of the same order of magnitude as the rates of collisions with electrons, while, for transitions with higher energies, the electron collisions are much more efficient than the hydrogen ones. An ion pair production in collisions with H I is much more efficient than an ionization in collisions with electrons in the entire range of energies. However, this does not affect the results, because the statistical equilibrium of O I in the range of parameters under consideration is determined by the bound-bound transitions. We performed a test calculation for the Sun neglecting ion-pair formation and mutual neutralization processes in collisions with hydrogen atoms and obtained very small changes in level populations that led to changes in the non-LTE abundance within 0.003 dex for the O I 7771-5 Å lines.

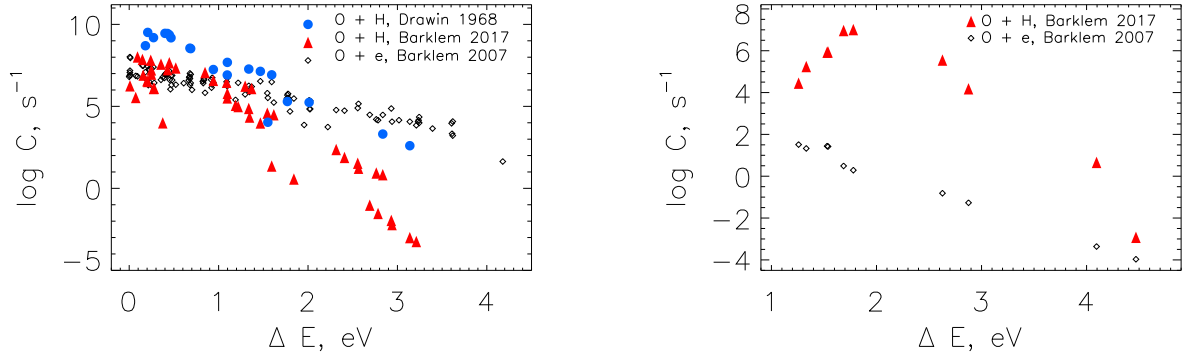


Figure 1: Left panel: Excitation rates in collisions with electrons (diamonds) and hydrogen atoms, according to the quantum-mechanical calculations of Barklem (2018) (triangles) and the approximation of Drawin (1968) (circles), versus transition energy. Right panel: The rates of the processes  $\text{O I} + e^- \leftrightarrow \text{O II} + 2e^-$  (diamonds) and  $\text{O I} + \text{H I} \leftrightarrow \text{O II} + \text{H}^-$  (triangles). The rates were calculated for the density of hydrogen atoms  $\log N_H = 17$ , the electron density  $\log N_e = 14$ , and the temperature  $T = 6840$  K.

### 3 Analysis of O I lines in the solar spectrum

The solar abundance was determined using the spectrum of the Sun as a star (Kurucz et al. 1984). The model atmosphere has an effective temperature  $T_{\text{eff}} = 5780$  K, surface gravity  $\log g = 4.44$ , and microturbulent velocity  $\xi_t = 0.9 \text{ km s}^{-1}$ . We use the classical 1D models from the MARCS grid (Gustafsson et al. 2008).

The list of lines and the derived oxygen abundance are given in Table 1. The atomic data for transitions, i.e., the wavelength  $\lambda$ , the oscillator strength ( $\log gf$ ), and excitation energy of the lower level ( $E_{\text{exc}}$ ), were taken from the VALD database (Kupka et al. 1999; Ryabchikova et al. 2015).

The application of accurate data for collisions with hydrogen atoms led to an increase in the departures from LTE and a strengthening of the IR lines. We obtained the mean non-LTE oxygen abundance  $\log \varepsilon(\text{O}) = 8.69 \pm 0.08$ , which is lower than that derived in non-LTE with Drawinian rates by 0.07 dex. For the IR triplet lines in the Sun, the non-LTE abundance decreased by 0.11 dex. For the 8446 Å lines the change is slightly smaller, 0.07 dex. In comparison with our previous results (Sitnova et al. 2013), the difference between the non-LTE abundances from the 7771-5 and 8446 Å lines increased from 0.02 to 0.05 dex. For the weak 6158 and 6300 Å lines in the visible range, the departures from LTE are still negligible, irrespective of the method of calculating the inelastic collisions with hydrogen atoms. The difference of 0.07 dex between the non-LTE abundances from the forbidden [O I] 6300 Å line and the 7771-5 Å lines obtained in our previous paper decreased to 0.04 dex. The difference in non-LTE abundances from the 6158 and 7771-5 Å lines increased from 0.07 to 0.18 dex. It should be noted that the abundance from the 6158 Å line is systematically higher than that from the IR triplet not only for the Sun but also for FG dwarfs. According to the data from Zhao et al. (2016), the mean difference  $\Delta = 0.12 \pm 0.07$  is obtained by comparing the absolute non-LTE abundances from these two lines for 17 FG stars in the [Fe/H] range from -0.8 to 0.2. With the classical MARCS model atmosphere Asplund et al. (2004) obtained a difference of 0.13 dex in the non-LTE abundance between these two lines for the Sun. The systematic difference is probably caused by the inaccuracy of the oscillator strengths calculated theoretically by Hibbert et al. (1991).

It is worth noting that using 3D non-LTE line formation calculations with O I + H I rate coefficients from Barklem (2018), Amarsi et al. (2018) derived  $\log \varepsilon(\text{O}) = 8.69 \pm 0.03$  from the O I 7771-5 Å lines. Our NLTE modelling with classical 1D model atmosphere gives average non-LTE abundance from the IR triplet lines,  $\log \varepsilon(\text{O}) = 8.65 \pm 0.03$ , which is consistent within the error bars with those derived by Amarsi et al. (2018).

## 4 Oxygen abundance in the sample stars

In this section, we redetermine the non-LTE oxygen abundance based on an improved model atom for 46 FG stars investigated by us previously (Zhao et al. 2016).

### 4.1 Stellar sample, observations, and atmospheric parameters

The sample of stars includes 46 unevolved stars, from dwarfs to subgiants. The stars are uniformly distributed in metallicity over a wide range,  $-2.6 < [\text{Fe}/\text{H}] < 0.2$ . High-resolution ( $\lambda/\Delta\lambda > 45\,000$ ) spectra with a signal-to-noise ratio  $S/N > 60$  were obtained at the 3-m telescope of the Lick Observatory with the Hamilton spectrograph or taken from the UVES<sup>5</sup> and ESPaDOnS<sup>6</sup> archives. We also used the spectra obtained at the 2.2-m telescope of the Calar Alto Observatory with the FOCES spectrograph and provided by K. Fuhrmann. The

---

<sup>5</sup>[http://archive.eso.org/eso/eso\\_archive\\_main.html](http://archive.eso.org/eso/eso_archive_main.html)

<sup>6</sup><http://www.cadc-ccda.hia-ihp.nrc-cnrc.gc.ca/en/search/>

Table 1: The list of O I lines with atomic parameters and LTE and non-LTE solar abundances. The non-LTE abundance is given for the cases where the inelastic collisions with hydrogen atoms were calculated from the approximate formula (S13) and based on the quantum-mechanical calculations (S17)

$\lambda$ , Å	$E_{exc}$ , eV	log gf	transition	LTE	non-LTE, S13	non-LTE, S17
6158.146	10.741	-1.841	$3p^5P - 4d^5D^\circ$	8.83	8.82	8.82
6158.176	10.741	-0.996	$3p^5P - 4d^5D^\circ$	8.83	8.82	8.82
6158.186	10.741	-0.409	$3p^5P - 4d^5D^\circ$	8.83	8.82	8.82
6300.304	0.000	-9.720 <sup>1</sup>	$2p^3P - 2p^1D$	8.68	8.68	8.68
7771.941	9.146	0.369	$3s^5S^\circ - 3p^5P$	8.91	8.74	8.63
7774.161	9.146	0.223	$3s^5S^\circ - 3p^5P$	8.91	8.76	8.65
7775.390	9.146	0.001	$3s^5S^\circ - 3p^5P$	8.87	8.75	8.66
8446.250	9.521	-0.463	$3s^3S^\circ - 3p^3P$	8.87	8.77	8.70

1 – The data from Froese Fisher et al. (1998).

When fitting the [O I] 6300 Å line, we took into account the blending Ni I 6300.34 line with  $\log(gf) = -2.11$  (Johansson et al. 2003) and the abundance  $\log \varepsilon(\text{Ni}) = 6.23$ .

observations and their reduction were described in detail by Sitnova et al. (2015), Pakhomov and Zhao (2013), and Zhao et al. (2016).

We use the atmospheric parameters carefully investigated by various methods in Sitnova et al. (2015). For the majority of stars, there are effective temperature determinations by the infrared flux method (Alonso 1996; Casagrande et al. 2010, 2011); the effective temperature for each star can be estimated from its color indices. The adopted temperatures agree with the photometric ones within the errors of determination and were chosen so as to provide agreement between the non-LTE abundances from Fe I and Fe II lines. For ten stars of our sample, there are  $T_{\text{eff}}$  determinations based on the bolometric fluxes and the angular diameters measured with the CHARA interferometer (Boyajian et al. 2012, 2013; North et al. 2009; von Braun et al. 2014). Our temperatures are systematically higher than the interferometric ones by  $78 \pm 81$  K. However, this difference does not exceed the error in  $T_{\text{eff}}$ , which we estimate to be 80 K. For two other stars, HD 140283 and HD 103095, the interferometric temperatures measured previously by Creevey et al. (2012, 2015) and Boyajian et al. (2013) differ from those adopted by us by more than 250 K. Karovicova et al. (2018) redetermined the angular diameters and bolometric fluxes for these two stars, which led to an increase in  $T_{\text{eff}}$  and agreement with our determinations within 10 K.

The Hipparcos trigonometric parallaxes (van Leeuwen et al. 2007) are available for all sample stars, which allows to calculate  $\log g$  by a spectroscopy-independent method. For the stars where the Hipparcos parallax error exceeds 10%, surface gravities were refined by analyzing the non-LTE abundances from Fe I and Fe II lines. The statistical equilibrium of Fe I–II was calculated with the model atom developed by Mashonkina et al. (2011) with the

scaling factor to the Drawin rates of inelastic collisions with hydrogen atoms  $S_{\text{H}} = 0.5$ . It is worth noting that, in the first Gaia<sup>7</sup> data release (DR1), parallaxes for 22 stars of our sample became available (Brown et al. 2016). We achieved good agreement between our spectroscopic  $\log g$  and those calculated from the Gaia DR1 parallaxes:  $\Delta \log g(\text{Spec} - \text{Gaia}) = -0.01 \pm 0.07$ , despite the fact that for the same 22 stars the spectroscopic  $\log g$  differ noticeably from those derived from the Hipparcos data,  $\Delta \log g(\text{Spec} - \text{Hipparcos}) = -0.15 \pm 0.12$ . The differences between  $\log g_{\text{spec}}$  and  $\log g_{\text{Hipp}}$  concern the stars that are 100 pc or more away from the Sun. For the nearest stars, the spectroscopic  $\log g$  agree well with those calculated from both Hipparcos and Gaia DR1 data.

The microturbulent velocity  $\xi_t$  and  $[\text{Fe}/\text{H}]$  were derived from Fe I and Fe II lines, respectively. Additionally,  $T_{\text{eff}}$ ,  $\log g$ , and  $[\text{Fe}/\text{H}]$  were checked using a grid of evolutionary tracks from Yi et al. (2001). The stars sit on the evolutionary tracks corresponding to their mass, age, and metallicity.

## 4.2 Influence of inelastic collisions with hydrogen atoms on the non-LTE oxygen abundance depending on atmospheric parameters

The non-LTE and LTE oxygen abundances for the sample stars were derived in our earlier study (Zhao et al., 2016). Here, we redetermined the non-LTE oxygen abundance from the IR 7771-5 Å triplet lines using the quantum-mechanical data for inelastic collisions with hydrogen atoms. The mean difference between the non-LTE abundances from the triplet lines obtained in this and the previous paper is shown for each of 46 stars in Fig. 2 as a function of metallicity, effective temperature, and surface gravity.

Just as for the Sun, the application of accurate data for the sample stars leads to a lower non-LTE oxygen abundance. The difference in non-LTE abundance ranges from 0.02 to 0.15 dex, depending on the atmospheric parameters. The difference between the non-LTE abundances derived with accurate and approximate data diminishes with decreasing metallicity, because, in metal-poor stars, the O I lines are weak and the non-LTE corrections are small in absolute value.

## 4.3 The Galactic $[\text{O}/\text{Fe}]$ trend

Figure 3 shows the derived  $[\text{O}/\text{Fe}]$  ratio together with those from our previous paper (Zhao et al. 2016). In the metallicity range  $-1 < [\text{Fe}/\text{H}] < 0.2$ , the  $[\text{O}/\text{Fe}]$  ratio for each star changed within 0.03 dex compared to the previous results. For these stars, the shift in  $[\text{O}/\text{Fe}]$  is minor, since the change in the oxygen non-LTE abundance is approximately the same as that for the Sun. For stars with  $[\text{Fe}/\text{H}] < -1$ , the  $[\text{O}/\text{Fe}]$  ratio turns out to be higher than the previous value, and  $[\text{O}/\text{Fe}]$  increasing trend with decreasing  $[\text{Fe}/\text{H}]$  became prominent. This happens, because, for stars with  $[\text{Fe}/\text{H}] < -1$ , the change in the oxygen non-LTE abundance is smaller in absolute value than those for the Sun and it decreases with decreasing  $[\text{Fe}/\text{H}]$ .

---

<sup>7</sup><https://www.cosmos.esa.int/gaia>



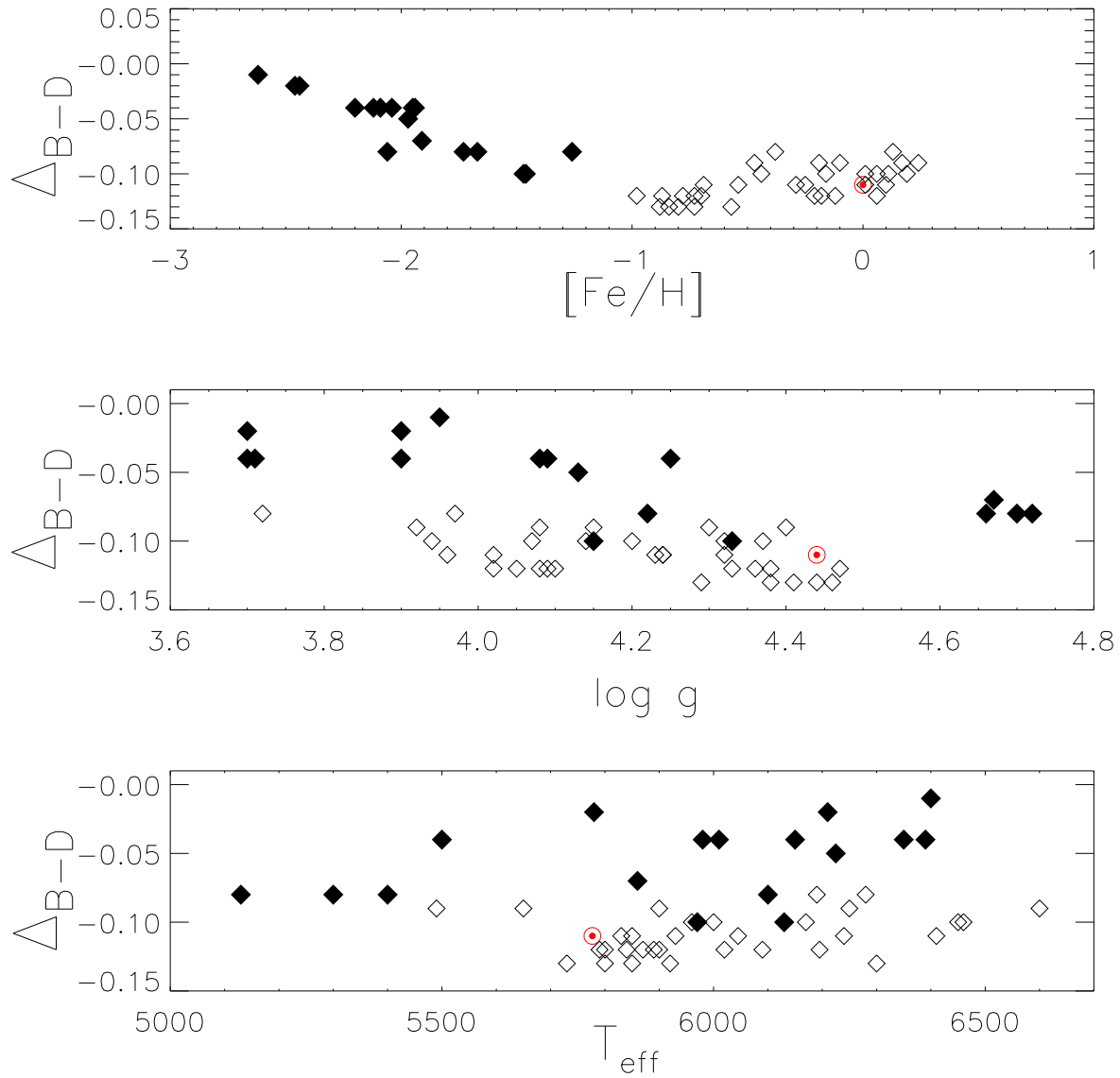


Figure 2: The mean difference between the non-LTE abundances from the triplet lines derived with accurate and approximate data for collisions with hydrogen atoms ( $\Delta_{B-D}$ ) is shown for 46 sample stars and the Sun as a function of atmospheric parameters. The filled and open symbols indicate the stars with  $[\text{Fe}/\text{H}] < -1$  and  $[\text{Fe}/\text{H}] > -1$ , respectively.

Among the modern Galactic chemical evolution models, a model of Kobayashi et al. (2011) fits our previous data for  $[\text{O}/\text{Fe}]$  best of all. This model predicts a slow decrease in  $[\text{O}/\text{Fe}]$  from 0.7 to 0.6 as  $[\text{Fe}/\text{H}]$  increases from  $-3$  to  $-1$  and then a sharp drop in  $[\text{O}/\text{Fe}]$  down to 0.1 at  $[\text{Fe}/\text{H}] = -0.17$  (the values were recalculated by taking into account the difference between our previous solar oxygen and iron abundances and those adopted by Kobayashi et al. (2011)). The revision of the oxygen abundance led to an increase in  $[\text{O}/\text{Fe}]$  with decreasing metallicity at  $[\text{Fe}/\text{H}] < -1$  instead of a plateau at  $[\text{O}/\text{Fe}] = 0.6$ , as derived in our previous study. The rising trend in  $[\text{O}/\text{Fe}]$  with decreasing  $[\text{Fe}/\text{H}] < -1$  can be qualitatively described by the model of Kobayashi et al. (2011), where rapidly rotating metal-poor massive stars were taken into account. Including rapidly rotating massive stars improves significantly the description of the observed behavior of  $[\text{C}/\text{Fe}]$  and  $[\text{N}/\text{Fe}]$  at  $[\text{Fe}/\text{H}] < -1.5$ , but does not affect the behavior of heavier elements. The model predicts oxygen abundance of  $\log \varepsilon = 8.93$  at  $[\text{Fe}/\text{H}] = 0$  and fits the determinations of Anders and Grevesse (1989) for the Sun. In absolute scale, this model fits well the data from Zhao et al. 2016 at  $[\text{Fe}/\text{H}] < -1$ , while the predicted  $[\text{O}/\text{Fe}]$  is larger than the observed at  $-1 < [\text{Fe}/\text{H}] < 0.2$ . The current revision in solar and stellar oxygen abundance leads to a discrepancy between model predictions and observations throughout all metallicity regimes.

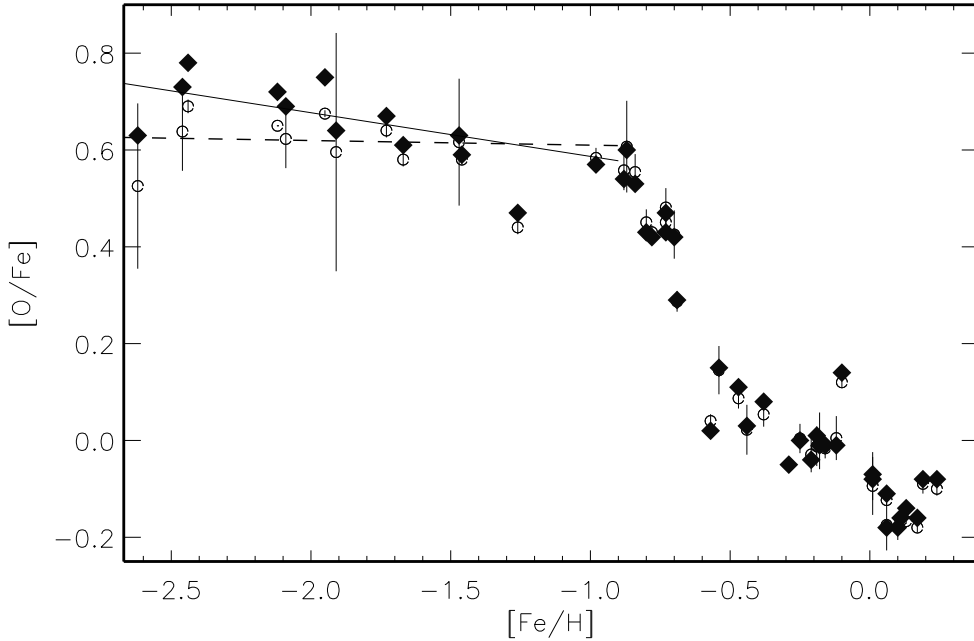


Figure 3: The  $[\text{O}/\text{Fe}]$  ratio derived in non-LTE with the accurate (diamonds) and approximate (circles) rates of inelastic collisions with hydrogen atoms is shown for 46 sample stars as a function of  $[\text{Fe}/\text{H}]$ . The straight lines  $[\text{O}/\text{Fe}] = 0.60 - 0.01[\text{Fe}/\text{H}]$  (dashed) and  $[\text{O}/\text{Fe}] = 0.50 - 0.09[\text{Fe}/\text{H}]$  (solid) indicate the linear interpolation result in the range  $-2.6 < [\text{Fe}/\text{H}] < -1.3$ . We excluded the star HD 103095 with  $[\text{Fe}/\text{H}] = -1.26$  when calculating the slopes of the straight lines, because it belongs to the type of low- $\alpha$  stars.

## 5 Conclusions

We performed non-LTE calculations for O I using the data from Barklem (2018) for collisions with hydrogen atoms. The non-LTE abundances from the O I lines were determined for the Sun and 46 FG stars in a wide metallicity range,  $-2.6 < [\text{Fe}/\text{H}] < 0.2$ .

The application of accurate data leads to a strengthening of the departures from LTE and a decrease in the abundance from the IR lines. The largest changes in the non-LTE abundance we found for the IR 7771-5 Å triplet lines. For the Sun, the non-LTE abundance from these lines decreases by 0.11 dex compared to what is obtained with approximate data for collisions with hydrogen atoms. Our new calculations do not affect the non-LTE abundance from weak lines in the visible range (6158, 6300 Å).

For the Sun, we obtained the mean non-LTE oxygen abundance  $\log \varepsilon(\text{O}) = 8.69 \pm 0.08$ , which is lower than that inferred in non-LTE with approximate data for collisions with hydrogen atoms by 0.07 dex. This value is even farther from what is required to reconcile the theoretical and observed density and sound speed profiles.

For 46 stars of the sample, the changes in the non-LTE abundance vary from 0.02 to 0.13 dex, depending on the atmospheric parameters. The change in the solar oxygen abundance and the oxygen abundance for individual stars led to a change in the behavior of the Galactic [O/Fe] trend with [Fe/H] in the range  $-2.6 < [\text{Fe}/\text{H}] < -1$ : the increase in [O/Fe] with decreasing [Fe/H] became more noticeable. For stars with  $-1 < [\text{Fe}/\text{H}] < 0.2$ , the changes in the non-LTE abundance for the sample stars are close to what was obtained for the Sun. Therefore, the [O/Fe] ration barely changed. The refined [O/Fe] trend can be used for testing of Galactic chemical evolution models.

**Acknowledgments:** This work was supported by the Russian Science Foundation (grant no. 17-13-01144). We are grateful to K. Fuhrmann for the spectra and O. Kochukhov for the binmag code. We made use the VALD and MARCS databases. This study is based on observations made with ESO Telescopes at the La Silla Paranal Observatory and at the Canada-France-Hawaii Telescope (CFHT), which is operated by the National Research Council (NRC) of Canada, the Institut National des Science de l’Univers of the Centre National de la Recherche Scientifique (CNRS) of France, and the University of Hawaii. The operations at the CFHT are conducted with care and respect from the summit of Maunakea, which is a significant cultural and historic site. This work has made use of data from the European Space Agency (ESA) mission *Gaia* (<https://www.cosmos.esa.int/gaia>), processed by the *Gaia* Data Processing and Analysis Consortium (DPAC, <https://www.cosmos.esa.int/web/gaia/dpac/consortium>). Funding for the DPAC has been provided by national institutions, in particular the institutions participating in the *Gaia* Multilateral Agreement.

## References

- [1] C. Allende Prieto, M. Asplund, P. Fabiani Bendicho, *Astron. Astrophys.*, **423**, 1109 (2004);
- [2] A. M. Amarsi, M. Asplund, R. Collet, J. Leenaarts, *MNRAS*, 454, L11 (2015)

- [3] A. Alonso, S. Arribas, C. Martinez-Roger, *Astrophys. J. Suppl. Ser.*, 117, 227 (1996)
- [4] A. M. Amarsi, P. S. Barklem, M. Asplund, R. Collet, and O. Zatsarinny, ArXiv e-prints, 1803.10531 (2018);
- [5] E. Anders and N. Grevesse, *Geochimica et Cosmochimica Acta*, vol. 53, 197, (1989);
- [6] M. Arnaud, R. Rothenflug, *Astron. Astrophys.*, **60**, 425 (1985);
- [7] M. Asplund, N. Grevesse, A. J. Sauval, C. Allende Prieto, D. Kiselman, *Astron. Astrophys.*, **417**, 751 (2004);
- [8] M. Asplund, N. Grevesse, A. J. Sauval, P. Scott, *Astron. Astrophys.*, **481**, 522 (2009);
- [9] John N. Bahcall and Aldo M. Serenelli, *Astrophys. J.*, **626**, 530 (2005);
- [10] P. S. Barklem, *Astron. Astrophys.*, **462**, 781 (2007);
- [11] P. S. Barklem, *Phys. Rev. A*, **93**, 042705 (2016);
- [12] P. S. Barklem, *Astron. Astrophys.*, 610, id.A57, 7 (2018);
- [13] P. S. Barklem, A. K. Belyaev, A. S. Dickinson, F. X. Gadea, *Astron. Astrophys.*, **519**, A20 (2010);
- [14] P. S. Barklem, A. K. Belyaev, A. Spielfiedel, M. Guitou, N. Feautrier, *Astron. Astrophys.*, **541**, A80 (2012);
- [15] K. Butler, J. Giddings, *Newsletter on Analysis of Astronomical Spectra* 9, University of London, **723**, (1985);
- [16] A. K. Belyaev, *Astron. Astrophys.*, 560, A66, 062703, (2013)
- [17] A. K. Belyaev, & P. Barklem, *Phys.Rev.*, A68, 062703, (2003)
- [18] A. K. Belyaev, & S. A. Yakovleva, *Astron. Astrophys.*, **606**, A147 (2017)
- [19] A. K. Belyaev, P. S. Barklem, A. S. Dickinson, & F. X. Gadéa, *Phys. Rev. A*, 81, 032706, (2010)
- [20] A. K. Belyaev, J. Grosser, J. Hahne, & T. Menzel, *Phys.Rev.*, A60, 2151, (1999)
- [21] A. K. Belyaev, S. A. Yakovleva, P. S. Barklem, *Astron. Astrophys.*, **572**, T103 (2014)
- [22] A. K. Belyaev, S. A. Yakovleva, M. Guitou, A. O. Mitrushchenkov, A. Spielfiedel, N. Feautrier, *Astron. Astrophys.*, 587, A114, (2016)
- [23] T. Bensby, S. Feltzing, M. S. Oey, *Astron. Astrophys.*, 562, A71 (2014)

- [24] S. Bertran de Lis, C. Allende Prieto, S. R. Majewski, R. P. Schiavon, J. A. Holtzman, M. Shetrone, R. Carrera, A. E. García Pérez, et al., *Astron. Astrophys.*, **590**, A74 (2016);
- [25] T. S. Boyajian, H. A. McAlister, G. van Belle, D. R. Gies, T. A. ten Brummelaar, K. von Braun, C. Farrington, P. J. Goldfinger et al., *Astrophys. J.*, **746**, 101 (2012);
- [26] T. S. Boyajian, K. von Braun, G. van Belle, C. Farrington, G. Schaefer, J. Jones, R. White, H. A. McAlister et al., *Astrophys. J.*, **771**, 40 (2013);
- [27] K. von Braun, T. S. Boyajian, G. T. van Belle, S. R. Kane., J. Jones, C. Farrington, G. Schaefer, N. Vargas et al., *MNRAS*, **438**, 2413 (2014);
- [28] M. Carlsson and P. G. Judge, *Astrophys. J.*, **402**, 344 (1993);
- [29] L. Casagrande, I. Ramírez, J. Meléndez, M. Bessell, M. Asplund, *Astron. Astrophys.*, 512, A54 (2010);
- [30] L. Casagrande, R. Schönrich, M. Asplund, S. Cassisi, I. Ramírez, J. Meléndez, T. Bensby, S. Feltzing, *Astron. Astrophys.*, 530, A138 (2011);
- [31] E. Caffau, H. G. Ludwig, M. Steffen, T. R. Ayres, P. Bonifacio, R. Cayrel, B. Freytag, B. Plez, *Astron. Astrophys.*, **488**, I3, 1031 (2008);
- [32] R. Cayrel, E. Depagne, M. Spite, V. Hill, F. Spite, *Astron. Astrophys.*, **416**, p.1117 (2004);
- [33] O. L. Creevey, F. Thevenin, T. S. Boyajian, P. Kervella, A. Chiavassa, L. Bigot, A. Merand, U. Heiter et al., *Astron. Astrophys.*, **545**, A17 (2012);
- [34] O. L. Creevey, F. Thevenin, P. Berio, U. Heiter, K. von Braun, D. Mourard, L. Bigot, T. S. Boyajian et al., *Astron. Astrophys.*, **575**, A26 (2015);
- [35] H.W. Drawin, *Z. Physik*, **211**, 404 (1968);
- [36] H.W. Drawin, *Z. Physik*, **225**, 483 (1969);
- [37] D. Fabbian, M. Asplund, P. S. Barklem, M. Carlsson, D. Kiselman, *Astron. Astrophys.*, **500**, 1221 (2009);
- [38] Froese Fisher and M. Saporov, G. Gaigalas, M. Godefroid, *Atomic data and nuclear data tables*, **70**, 119 (1998);
- [39] J. P. Fulbright, J. A. Johnson, *Astrophys. J.*, **595**, I2, p. 1154 (2003);
- [40] Gaia Collaboration, A. G. A. Brown, A. Vallenari, T. Prusti, J. H. J. de Bruijne, F. Mignard et al., *Astron. Astrophys.*, **595**, A2 (2016);
- [41] R. G. Gratton, E. Carretta, F. Matteucci, C. Sneden, *Astron. Astrophys.*, **358**, p.671 (2000);

- [42] B. Gustafsson, B. Edvardsson, K. Eriksson U. G., Jørgensen, Å. Nordlund, B. Plez, *Astron. Astrophys.*, **486**, 951 (2008);
- [43] A. Hibbert, E. Biemont, M. Godefroid, and N. Vaeck, *J. Phys.*, B 24, p. 3943 (1993);
- [44] H. Holweger, E.A. Mueller, *Solar Physics*, **39**, 19 (1974);
- [45] G. Israelian, R. J. Garcia Lopez, R. Rebolo, *Astrophys. J.*, **507**, I2, 805 (1998);
- [46] S. Johansson, U. Litzen, H. Lundberg, Z. Zhang, *Astrophys. J. L.*, **584**, L107 (2003);
- [47] H.R. Johnson, R.W. Milkey, L.W. Ramsey, *Astrophys. J.*, **187**, 147 (1974);
- [48] I. Karovicova, T. R. White, T. Nordlander, K. Lind, L. Casagrande, M. J. Ireland, D. Huber, O. Creevey et al., arXiv:1801.03274, 344 (2018);
- [49] Dan Kiselman, *Astron. Astrophys.*, **245**, L9 (1991);
- [50] C. Kobayashi, A. I. Karakas, H. Umeda, *MNRAS*, 414, 3231 (2011)
- [51] K. Kodaira and K. Tanaka, *Astron. Soc. Japan* 24, 355 (1972);
- [52] Kramida A., Ralchenko Y., Reader J., NIST ASD Team, NIST Atomic Spectra Database (version 5.3), available at <http://physics.nist.gov/asd>. National Institute of Standards and Technology, Gaithersburg, MD (2015);
- [53] F. Kupka, N.E. Piskunov, T.A. Ryabchikova, H. C. Stempels, W. W. Weiss, *Astron. Astrophys. Suppl.*, **138**, 119 (1999);
- [54] R. Kurucz, I. Furenlid, J. Brault, L. Testerman, *National Solar Observatory Atlas, Sunspot, New Mexico: National Solar Observatory* (1984);
- [55] F. van Leeuwen, *Astron. Astrophys.*, 474, 653 (2007)
- [56] L. Mashonkina, T. Gehren, J.R. Shi, A. J. Korn, F. Grupp, *Astron. Astrophys.*, **528**, A87 (2011);
- [57] A. Mitrushchenkov, M. Guitou, A. K. Belyaev, *J. Chem. Phys.*, **146**, 014304 (2017);
- [58] T. V. Mishenina, S. A. Korotin, V. G. Klochkova and V. E. Panchuk, *Astron. Astrophys.*, **353**, 978 (2000);
- [59] P. E. Nissen, F. Primas, M. Asplund and D. L. Lambert, *Astron. Astrophys.*, **390**, 235 (2002);
- [60] J. R. North, J. Davis, J. G. Robertson, T. R. Bedding, H. Bruntt, M. J. Ireland, A. P. Jacob, S. Lacour et al., *MNRAS*, **393**, 245 (2009);
- [61] E. Paunzen, I. Kamp, I. Kh. Iliev, U. Heiter, M. Hempel, W.W. Weiss, I.S. Barzova, F. Kerber et al., *Astron. Astrophys.*, **345**, 597 (1999);

- [62] Y. V. Pakhomov, G. Zhao, *Astrophys. J.*, 146, 97 (2013)
- [63] T. M. D. Pereira, M. Asplund, D. Kiselman., *Astron. Astrophys.*, **508**, 1403 (2009);
- [64] N. Przybilla, K. Butler, S. R. Becker, R. P. Kudritzki, K. A. Venn, *Astron. Astrophys.*, **359**, 1085 (2000);
- [65] I. Ramírez, C. Allende Prieto, D. L. Lambert, *Astrophys. J.*, 764, 78 (2013)
- [66] Johannes Reetz, *Astrophysics and Space Science.* , **265**, 171 (1999);
- [67] Henry van Regemorter, *Astrophys. J.*, **136**, 906 (1962);
- [68] T. Ryabchikova, N. Piskunov, Y. Pakhomov, V. Tsymbal, A. Titarenko, T. Sitnova, S. Alexeeva, L. Fossati, et al., *MNRAS*, **456**, 1221 (2016);
- [69] T. Ryabchikova, N. Piskunov, R. L. Kurucz, H. C. Stempels, U. Heiter, Y. Pakhomov, P. S. Barklem, *Phys. Scr.*, 90, 054005 (2015)
- [70] T. Sitnova, *Astron. Lett.*, **42**, 11, p. 734 (2016);
- [71] T. M. Sitnova, L. I. Mashonkina, and T. A. Ryabchikova, *Astron. Lett.* 39, 126 (2013);
- [72] T. Sitnova, G. Zhao, L. Mashonkina, Y. Chen, F. Liu, Y. Pakhomov, K. Tan, M. Bolte, et al., *Astrophys. J.*, 808, 148 (2015)
- [73] M. J. Seaton, *Atomic and Molecular Processes*, ed. D. R. Bates, 375 (1962);
- [74] M. J. Seaton, Y. Yan, D. Mihalas, A. K. Pradhan, *MNRAS*, **266**, 805 (1994);
- [75] W. Steenbock, H. Holweger, *Astron. Astrophys.*, **130**, 319 (1984);
- [76] N. G. Shchukina, *Kinem. Fiz. Neb. Tel* **3**, 36 (1987);
- [77] Yoichi Takeda, *Astronomical Society of Japan* **44**, 3, 309 (1992);
- [78] J. Tomkin, M. Lemke, D. L. Lambert, C. Sneden, *Astron. J.*, **104**, 4, p. 1568 (1992);
- [79] V. Tsymbal, in S. J. Adelman, F. Kupka, W. W. Weiss, eds, *M.A.S.S., Model Atmospheres and Spectrum Synthesis Vol. 108 of Astronomical Society of the Pacific Conference Series, STARSP: A Software System For the Analysis of the Spectra of Normal Stars.* p. 198 (1996)
- [80] R. Wooley, C. W. Allen, *Monthly Notices of the Royal Astronomical Society*, **108**, 292 (1948);
- [81] S. Yi, P. Demarque, Y.-C. Kim, Y.-W. Lee, C. H. Ree, T. Lejeune, S. Barnes, *Astrophys. J. Suppl. Ser.*, 136, 417 (2001);
- [82] G. Zhao, L. Mashonkina, S. Alexeeva, Yu. Pakhomov, J.-R. Shi, T. Sitnova, K. Tan, H.-W. Zhang, et al., *Astrophys. J.*, **833**, I2, 225 (2016)